Circulation: Cardiovascular Interventions

ORIGINAL ARTICLE

Optimal Predilatation Treatment Before Implantation of a Magmaris Bioresorbable Scaffold in Coronary Artery Stenosis: The OPTIMIS Trial

Kirstine Nørregaard Hansen, MD; Jens Trøan, MD; Akiko Maehara, MD; Manijeh Noori, MD; Mikkel Hougaard, MD, PhD; Julia Ellert-Gregersen, MD, PhD; Karsten Tange Veien, MD; Anders Junker, MD, PhD; Henrik Steen Hansen, MD; Jens Flensted Lassen, MD, PhD; Lisette Okkels Jensen, MD, DMSci, PhD

BACKGROUND: Bioresorbable scaffolds (BRS) were developed to overcome limitations related to late stent failures of drug-eluting stents, but lumen reductions over time after implantation of BRS have been reported. This study aimed to investigate if lesion preparation with a scoring balloon compared with a standard noncompliant balloon minimizes lumen reduction after implantation of a Magmaris BRS assessed with optical coherence tomography and intravascular ultrasound.

METHODS: Eighty-two patients with stable angina were randomized in a ratio of 1:1 to lesion preparation with a scoring balloon versus a standard noncompliant balloon before implantation of a Magmaris BRS. The primary end point was minimal lumen area at 6-month follow-up.

RESULTS: Following Magmaris BRS implantation, minimal lumen area (6.4±1.6 versus 6.3±1.5 mm^2; P=0.65), mean scaffold area (7.8±1.5 versus 7.5±1.7 mm^2; P=0.37), and mean lumen area (8.0±1.6 versus 7.7±2.1 mm^2; P=0.41) did not differ significantly in patients with lesions prepared with scoring versus standard noncompliant balloon, respectively. Six-month angiographic follow-up with optical coherence tomography and intravascular ultrasound was available in 74 patients. The primary end point, 6-month minimal lumen area, was significantly larger in lesions prepared with a scoring balloon compared with a standard noncompliant balloon (4.7±1.4 versus 3.9±1.9 mm^2; P=0.04), whereas mean lumen area (7.2±1.4 versus 6.8±2.2 mm^2; P=0.35) did not differ significantly. Intravascular ultrasound findings showed no difference in mean vessel area at the lesion site from baseline to follow-up in the scoring balloon group (16.8±2.9 versus 17.0±3.6 mm^2; P=0.62), whereas mean vessel area (17.1±4.4 versus 15.7±4.9 mm^2; P<0.001) was smaller in lesions prepared with a standard noncompliant balloon due to negative remodeling.

CONCLUSIONS: Lesion preparation with a scoring balloon before implantation of a Magmaris BRS resulted in a significantly larger minimal lumen area after 6 months due to less negative remodeling compared with lesion preparation with a standard noncompliant balloon.

REGISTRATION: URL: https://www.clinicaltrials.gov; Unique identifier: NCT04666584.

GRAPHIC ABSTRACT: A graphic abstract is available for this article.

Key Words: absorbable implants ■ angina, stable ■ drug-eluting stents ■ tomography, optical coherence ■ ultrasonography, interventional

See Editorial by Alfonso et al

Correspondence to: Kirstine Nørregaard Hansen, MD, Department of Cardiology, Odense University Hospital, Sdr. Boulevard 29, 5000 Odense C, Denmark. Email kirstinenoerregaard@live.dk

Supplemental Material is available at https://www.ahajournals.org/doi/suppl/10.1161/CIRCINTERVENTIONS.124.014665.
For Sources of Funding and Disclosures, see page 45.

Circulation: Cardiovascular Interventions is available at www.ahajournals.org/journal/circinterventions

WHAT IS KNOWN

- The magnesium-based bioresorbable Magmaris scaffold is considered safe and efficient in the treatment of coronary artery stenosis, but lumen reductions over time have been observed during degradation.

WHAT THE STUDY ADDS

- Lesions preparation with a scoring balloon is safe and ensures less lumen reduction, better vascular healing, and less negative remodeling after implantation of a Magmaris bioresorbable scaffold compared with lesion preparation with a standard noncompliant balloon.
- Optimal lesion preparation should be considered before implantation of magnesium-based Magmaris bioresorbable scaffold.

Nonstandard Abbreviations and Acronyms

BIOSOLVE-II	Biotroniks – Safety and Performance in de Novo Lesion of Native Coronary Arteries With Magmaris
BRS	bioresorbable scaffold
DES	drug-eluting stents
EEM	external elastic membrane
IVUS	intravascular ultrasound
MAGSTEMI	Magnesium-Based Bioresorbable Scaffold in ST-Segment–Elevation Myocardial Infarction
MLA	minimal lumen area
MgBRS	magnesium-based Magmaris bioresorbable scaffold
OCT	optical coherence tomography
OPTIMIS	Optimal Predilatation Treatment Before Implantation of a Magmaris Bioresorbable Scaffold in Coronary Artery Stenosis
PCI	percutaneous coronary intervention

Bioresorbable scaffolds (BRS) were developed to provide temporary vessel support during the early phases of coronary vessel healing, leaving the artery stent-free after degradation as an alternative to drug-eluting stents (DES) during percutaneous coronary intervention (PCI).[1,2] The potential advantages of BRS were restored vasomotion and potential reduction in late stent failures. The Absorb everolimus-eluting BRS (Abbott Vascular, Abbott Park, IL) showed increased risk of scaffold thrombosis and vessel shrinkage over time[3] with significant minimal lumen area (MLA) reduction after 6 months assessed with optical coherence tomography (OCT).[4] It is hypothesized that the mechanism behind lumen reduction is based on decreased radial strength in BRS compared with bare-metal stents and the risk of recoil and scaffold dismantling.[5] The construction of BRS continued to develop, and different types are now available on the market. The magnesium-based BRS (Magmaris, Biotronik, Bülach, Switzerland; MgBRS) was later introduced with improved radial strength, a stronger backbone, a change in drug-polymer coating, and showed promising efficacy and long-term sustained safety.[6–9] Head-to-head comparison between newer generation DES and the MgBRS is limited, but the anti-restenotic efficacy has not yet solved the scaffold failure.[5,10]

Optimal lesion preparation before implantation of a MgBRS appeared to facilitate optimal scaffold sizing and better expansion postprocedure in complex lesions,[11] but the effect of aggressive predilation on vessel and lumen changes over time is uncertain. Peri-procedural intravascular imaging is recommended during implantation of a MgBRS due to the lack of a radiolucent backbone. OCT is ideal to assess lumen contours,[12] whereas intravascular ultrasound (IVUS) provides information on the vessel wall and vessel remodeling over time.[13,14] The aim of this study was to assess whether a more aggressive lesion preparation with a scoring balloon compared with a standard noncompliant balloon before implantation of a MgBRS resulted in less lumen reduction MLA after 6 months.

METHODS

The data that support the findings of this study are available from the corresponding author upon reasonable request.

Study Design

The OPTIMIS study (Optimal Predilatation Treatment Before Implantation of a Magmaris Bioresorbable Scaffold in Coronary Artery Stenosis) was a prospective, randomized-controlled trial conducted at Odense University Hospital in Denmark from December 2020 to September 2023. The study compared lesion preparation with a scoring balloon to a standard noncompliant balloon before implantation of a MgBRS and the effect on lumen dimension in the scaffold-treated segment after 6 months. The patients were randomized to the 2 predilatation methods in a ratio of 1:1. The primary hypothesis of the OPTIMIS study was that intense lesion preparation with a scoring balloon before implantation for a MgBRS would result in a larger MLA after 6-month follow-up, compared with standard predilatation with a noncompliant balloon. A detailed description of the study design has previously been published.[15]

All patients provided written informed consent for trial participation before randomization. The study was approved by the Regional Committees on Health Research Ethics for Southern Denmark (Project-ID: S-20200114) and Danish Data Agency (Journal no.: 20/49900), and the trial was registered at ClinicalTrials.gov (NCT04666584).

Patient Population

Eighty-two patients with stable angina pectoris referred to PCI were enrolled in the study if they met the inclusion. Patients

were eligible if: (1) age was between 18 and 80 years, (2) they had stable angina pectoris, (3) the target lesion was in a native coronary artery, and (4) the vessel was suitable for treatment with MgBRS, complying with the scaffolds recommended limitations of coronary artery diameter between ≥2.75 and ≤4.0 mm measured with OCT or IVUS. Exclusion criteria are shown in Table S1. All patients were screened for protocol inclusion and exclusion criteria before enrollment. Patients underwent clinical and invasive imaging follow-up with OCT and IVUS at 6 months.

Antithrombotic Therapy

Patients were treated with aspirin 75 mg/d before the PCI procedure. On the day for the PCI, they received a loading dose of 600 mg clopidogrel. Patients were prescribed dual antiplatelet therapy with aspirin 75 mg/d and clopidogrel 75 mg/d for 6 months, followed by lifelong monotherapy with 75 mg of aspirin. Patients in Warfarin or novel oral anticoagulant were loaded with 600 mg of clopidogrel. If patients had been admitted and treated for an acute myocardial infraction within the last 12 months, patients kept their previously prescribed antithrombotic medication.

Devices

The metallic-based MgBRS contains a magnesium alloy with a bioresobable poly L-lactide acid polymer coated with sirolimus as an eluting drug released completely after 100 days. The strut thickness is 150 µm. The MgBRS is completely absorbed after 1 year.[16] The scaffold sizes were available in a diameter of 3.0 and 3.5 mm and lengths of 15, 20, and 25 mm.

The scoring balloon (ScoreFlex, OrbusNeich) catheter is a short monorail-type balloon catheter. It provides forced dilatation with a dual-wire semi-compliant balloon system, which facilitates local, safe, and controlled plaque modification at lower resolution pressure.

Procedure Strategy

The coronary stenosis was identified by the PCI operator's interpretation of the angiography and was treated with MgBRS in all patients. Patients received a dose of heparin (70 UI/kg) before the procedure. At the discretion of the operator, predilatation with a 2.0 mm balloon was allowed. Preinterventional imaging with OCT and IVUS was performed. The scaffold sizing was based on the external elastic membrane (EEM) diameters of the proximal and distal reference segments assessed with IVUS. If the EEM was visible in >180° of the cross-sectional area, the smaller EEM diameter rounded down to the nearest 0.5 mm was used to determine scaffold diameter. If the EEM was visible in <180°, the scaffold diameter was based on the lumen diameter.[17] Patients were allocated 1:1 to either lesion preparation with (1) a scoring balloon or (2) a standard noncompliant balloon. The lesion was predilated in a 1:1 balloon:artery ratio. Up-scaling to a 0.5 mm larger balloon was allowed if the predilatation goal was not achieved, as long as the balloon type corresponded to the randomization arm. The use of a semi- or noncompliant balloon was allowed in both arms at the PCI operator discretion for predilatation. The use of the scoring balloon was mandatory in patients allocated to the scoring balloon arm and only allowed in these patients. The predilatation goal was an angiographic residual stenosis of <20%. The lesion was then treated with implantation of a MgBRS, and inflation pressure was maintained for 30 seconds during implantation. Mandatory postdilatation was performed with a noncompliant balloon with the same size or maximally 0.5 mm larger than the implanted scaffold. Finally, intravascular imaging with OCT and IVUS of the scaffold-treated segment was performed and controlled by the PCI operator and an on-site OCT analyst. Optimization (if any) was performed at the operators' discretion. Additional intervention was allowed if there was (1) major under-expansion (minimal scaffold area <4.5 mm^2), (2) major malapposition (defined as strut >0.3 mm from the lumen wall for >3 mm), (3) presence of significant edge dissection, or (4) residual stenosis <5 mm proximal or distal to the scaffold (causing MLA <4 mm^2). Repeated OCT and IVUS of the final result were then performed. Blinding of the patient, PCI operator, or investigator to the predilatation technique was not possible during the index procedure.

Intravascular Imaging Acquisition

OCT and IVUS were performed at baseline and after 6 months of follow-up. The imaging procedures were preceded by administration of 200 µg of intracoronary nitroglycerin. OCT was performed with a frequency-domain OPTIS OCT system (Illumien OCT system; Abbott Vascular, Santa Clara, CA) using the Dragonfly Imaging catheter. The catheter was positioned 10 mm distally to the lesion or scaffold-treated segment, and the coronary artery was then flushed with 15 mL of contrast injection to clear the artery for blood during automated pullback at a rate of 20 mm/s over a distance of 75 mm. The IVUS system (Boston Scientific, Marlborough, MA) used a 40 MHz OptiCross 2.6 Fr catheter placed 10 mm distally to the lesion or scaffold-treated segment. Motorized IVUS pullbacks were performed with a pullback speed of 0.5 mm/s after intracoronary bolus of 200 µg nitroglycerin.

Intravascular Imaging Analysis

The intravascular imaging pullbacks were analyzed by 2 independent analysts who were both blinded to the predilatation technique during analysis. The baseline IVUS and OCT pullbacks were matched with the follow-up images using anatomic landmarks. OCT offline software (Offline Review Workstation; Abbott Vascular) was used for quantitative OCT analysis, and the commercially available program for computerized IVUS analysis, Echoplaque (INDEC Systems Inc, Santa Clara, CA), was used for IVUS analysis. The scaffold-treated segment was analyzed for every mm. Lumen dimensions at baseline and follow-up were measured: MLA, mean lumen area, lumen volume, and difference in MLA (follow-up MLA − baseline MLA). Quantitative analysis of scaffold was done using IVUS because IVUS showed better detection of scaffold remnants than OCT. Scaffold dimensions at baseline were measured: minimal scaffold area, mean scaffold area, minimum scaffold diameter, and scaffold volume. Scaffold malapposition was defined to be present when the distance between the abluminal surface of the strut and the luminal surface of the vessel wall exceeded the struts thickness of 150 µm. Major malapposition was defined as struts >0.3 mm from the lumen wall for >3 mm in length,[18] and the remaining were classified as minor. At baseline, malapposition area, distance, and volume were analyzed. At follow-up, visible struts or strut remnants

were categorized as covered embedded, covered protruding, or malapposed (Figure S1). A strut was categorized as malapposed if the abluminal border of the strut/remnant was separated from the lumen surface by a visible space exceeding 150 µm. The malapposition observations were matched from baseline to follow-up and divided into resolved, persistent, or late-acquired malapposition. If a scaffold contained both resolved and persistent malapposition at follow-up, it was summarized as persistent. To evaluate the effect of the predilatation method on remodeling at the specific lesion site, IVUS was used to identify the preprocedure MLA in the lesion. The lesion site was defined as 5 mm proximally and distally to MLA. The corresponding 10 mm segment was identified in IVUS pullback postprocedure and at 6-month follow-up using anatomic landmarks such as side branches, calcified plaques, and scaffold edges. Remodeling was defined as changes in mean EEM area in the lesion site and deemed significant if the mean EEM area changed >0.5 mm^2. Enlargement was defined as positive remodeling, and reduction in mean EEM area was defined as negative remodeling. Quantitative IVUS analysis included measurements of EEM, peri-scaffold plaque (EEM area – scaffold area), and total plaque area (EEM area – lumen area).

Statistical Analysis

Categorical data were presented as numbers and frequencies and compared using χ^2 test or Fisher exact statistics. Continuous data were presented as mean±SD and compared using Student *t* test. A paired *t* test was used for comparison from baseline to follow-up. If the distribution were skewed, the nonparametric Mann-Whitney *U* test was performed, and median with interquartile range was stated.

All tests were 2-tailed, and a $P<0.05$ was considered statistically significant. STATA, version 18.0 (StataCorp, Collage Station, TX), was used for the statistical analysis. Interobserver variability for imaging analysis was tested for consistency of agreement using an intraclass correlation coefficient calculated for MLA at follow-up and for malapposition area at baseline and follow-up. The Pearson correlation coefficient was used to evaluate the direction and strength of the linear relationship between 2 parameters.

The estimated sample size was based on data from the HONEST study (The Coronary Artery Healing Process After Bioresorbable Scaffold in Patients With Non–ST-Segment–Elevation Myocardial Infarction).[19] The reduction of MLA from 6.99 to 5.01 mm^2 (27%) 6 months after implantation of the Magmaris BVS represented the expected reference group. Optimal lesion preparation with predilatation with a scoring balloon is estimated to minimize MLA reduction from 6.99 to 6.22 mm^2 (11%). A power calculation is conducted using the expected MLA after 6 months (6.22 mm^2 for the scoring balloon and 5.01 mm^2 for the standard noncompliant balloon group with a SD of 1.80). Inclusion of 35 patients in each group is necessary to reach statistical significance in cases of 2-tailed significance level of 0.05 and power of 80%. Loss to follow-up and poor image quality finalize an expected dropout rate of 15%, thereby requiring 82 patients in total.

End Points

The primary end point was MLA in the scaffold-treated segment predilated with a scoring balloon versus a standard noncompliant balloon 6 months after implantation of a MgBRS assessed with OCT.

Secondary end points were differences between treatment groups in (1) change in MLA and (2) percentage and size of incomplete scaffold apposition at baseline and follow-up.

RESULTS

A flowchart of enrolled patients is provided in Figure 1.

In total, 82 patients were enrolled in the study. Follow-up images were not available in 8 patients due to the following reasons: 1 patient randomized to standard noncompliant balloon predilatation was excluded due to vessel dissection that could not be covered by a MgBRS scaffold. Two patients were excluded, 1 in the scoring balloon group and 1 in the standard noncompliant balloon group, due to scaffold failure where the MgBRS was lost in the coronary artery proximally to the study lesion. In all 3 cases, patients were treated with a DES. Five patients had unavailable follow-up images: 2 patients withdrew consents (1 in the scoring balloon group and 1 standard noncompliant balloon group), 1 patient died within the 6-month angiographic follow-up (standard noncompliant balloon group), 1 patient had a subacute scaffold thrombosis 5 days after implantation (standard noncompliant balloon group), and 1 patient was postponed due to nurses' strikes (standard noncompliant balloon group).

Clinical and Procedural Characteristics

Baseline clinical and procedural characteristics are presented in Table 1 and Table 2.

The treatment groups were well matched without any significant differences in baseline characteristics. Also, there were no significant differences in procedural characteristics, except for balloon length, which was significantly shorter in the scoring balloon group (only available in 10 and 15 mm; 15.0 mm [10.0; 15.0]) compared with the standard noncompliant balloon group (15.0 mm [15.0; 15.0], $P=0.004$). Postdilatation balloon diameter (scoring, 4.0 mm [3.5; 4.0] versus standard, 3.5 mm [3.5; 4.0]; $P=0.34$) and maximal pressure (scoring, 12.0 atm [12.0; 14.0] versus standard, 12.0 atm [12.0; 14.0]; $P=0.94$) were comparable between groups.

Optical Coherence Tomography Findings

Postprocedure and 6-month follow-up OCT findings are presented in Table 3. Interobserver variability for MLA at follow-up was: intraclass correlation coefficient of 0.996 (95% CI, 0.999–1.00; $P<0.001$), for total malapposition area at baseline: intraclass correlation coefficient of 0.949 (95% CI, 0.77–0.99; $P<0.001$), and for total malapposition at follow-up: intraclass correlation coefficient of 0.874 (95% CI, 0.50–0.97; $P=0.001$).

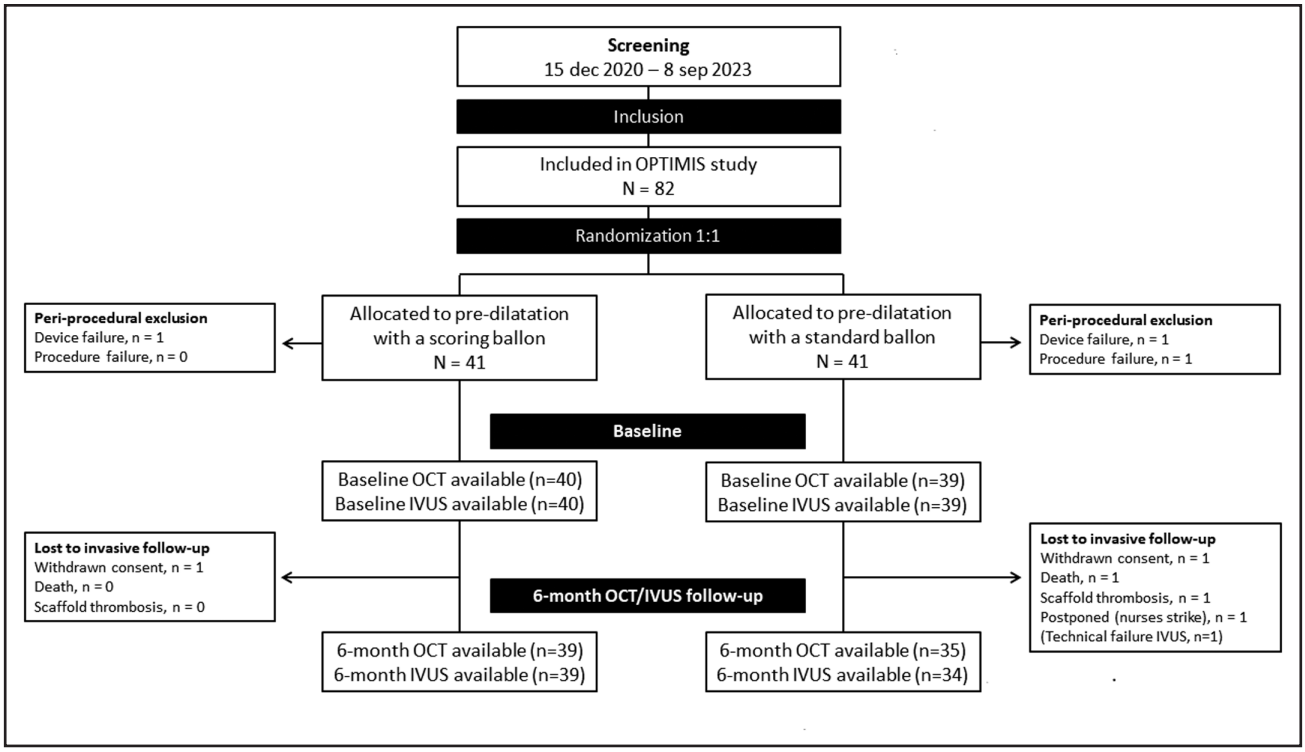

Figure 1. Flowchart.
IVUS indicates intravascular ultrasound; OCT, optical coherence tomography; and OPTIMIS, Optimal Predilatation Treatment Before Implantation of a Magmaris Bioresorbable Scaffold in Coronary Artery Stenosis.

Lumen Dimensions

At baseline, there was no significant difference in MLA, mean LA, or lumen volume between the 2 treatment groups assessed with OCT. At 6-month follow-up, MLA (the primary end point) in the scaffold-treated segment was significantly larger in the patients allocated to predilatation with a scoring balloon, compared with a standard noncompliant balloon (4.71±1.35 versus 3.91 ±1.86 mm^2; *P*=0.04). There was no significant difference between the 2 groups in mean LA or lumen volume at 6-month follow-up. There was a relative reduction in MLA of −24.8% for the scoring balloon group compared with −38.3% in the standard noncompliant balloon group, *P*=0.009. Representative cases of lumen reduction from baseline to follow-up are shown in Figure 2.

Table 1. Patient Baseline Characteristics

	Scoring balloon, n=41	Standard balloon, n=41	*P* value
Age, y	64.9±9.0	64.8±7.9	0.94
Male, n (%)	27 (65.9)	28 (68.3)	0.81
Family history of IHD, n (%)	19 (46.3)	17 (41.5)	0.66
History of smoking, n (%)			0.06
Current smoker	6 (14.6)	6 (14.6)	
Previous smoker	21 (51.2)	11 (26.8)	
Hypertension, n (%)	17 (41.5)	25 (61.0)	0.08
Hypercholesterolemia, n (%)	11 (26.8)	13 (31.7)	0.63
Diabetes, n (%)	4 (9.8)	8 (19.5)	0.21
Body mass index, kg/m^2	27.9±9.7	27.9±3.7	0.97
eGFR, mL/min	79.7±12.5	82.1±11.6	0.37
Previous myocardial infarction, n (%)	9 (22.0)	4 (9.8)	0.13
Previous PCI, n (%)	11 (26.8)	6 (14.6)	0.17
Previous CABG, n (%)	0 (0.0)	0 (0.0)	1.00

Data are shown as mean±SD. CABG indicates coronary bypass graft; eGFR, estimated glomerular filtration rate; IHD, ischemic heart disease; and PCI, percutaneous coronary intervention.

Scaffold Measurements and Malapposition

At baseline, scaffold parameters such as scaffold length, mean scaffold area, minimal scaffold area, and total scaffold volume were similar in the 2 groups. Total number of analyzable struts were similar at baseline between the 2 groups (199.9±70.5 in the scoring balloon group and 210.7±60.0 in the standard noncompliant balloon group; *P*=0.46). At follow-up, the total number of analyzable struts was reduced to 70.8±35.1 in the scoring balloon group and 85.1±32.1 in the standard noncompliant balloon group (*P*=0.07). There were similar percentages of protruding and embedded strut remnants at follow-up (scoring, 58.3±22.0% versus standard, 54.1±26.6%; *P*=0.47). There was a positive correlation between Δmean lumen area and percentage of protruding remnants (r=0.59, *P*<0.001) and a negative correlation

Table 2. Procedural and Angiographic Characteristics

	Scoring balloon, n=40	Standard balloon, n=39	*P* value
Target coronary artery, n (%)			0.77
Left anterior descending	23 (57.5)	24 (61.5)	
Left circumflex	5 (12.5)	6 (15.4)	
Right coronary artery	12 (30.0)	9 (23.1)	
Lesion length, mm	20.0 [20.0; 25.0]	20.0 [20.0; 25.0]	0.95
Reference vessel diameter, mm	3.5 [3.3; 3.5]	3.5 [3.0; 3.5]	0.14
Predilatation, n (%)	40 (100)	39 (100)	1.00
Balloon diameter at predilatation, mm	3.5 [3.0; 3.5]	3.5 [3.0; 3.5]	0.68
Balloon length at predilatation, mm	15.0 [10.0; 15.0]*	15.0 [15.0; 15.0]*	0.004
Max balloon pressure at predilatation, atm	12.0 [12.0; 14.0]	14.0 [12.0; 16.0]	0.05
No. of scaffolds per lesion, mm	1.1±0.3 1 [1; 1]	1.1±0.2 1 [1; 1]	0.42 0.42
Scaffold length, mm	20.0 [15.0; 25.0]	20.0 [20.0; 25.0]	0.37
Scaffold diameter, mm	3.5 [3.0; 3.5]	3.5 [3.0; 3.5]	0.31
Maximum balloon pressure, atm	12.0 [10.0; 14.0]	12.0 [10.0; 14.0]	0.92
Expected scaffold diameter, mm	3.5 [3.3; 3.7]	3.5 [3.1; 3.7]	0.59
Postdilatation, n (%)	37 (92.5)	39 (100.0)	0.08
Balloon diameter at postdilatation, mm	4.0 [3.5; 4.0]	3.5 [3.5; 4.0]	0.34
Balloon length at postdilatation, mm	15.0 [12.0; 15.0]	15.0 [15.0; 20.0]	0.24
Max balloon pressure at postdilatation, atm	12.0 [12.0; 14.0]	12.0 [12.0; 14.0]	0.94
Flouro time, min	11.9±4.9	11.7±5.1	0.89
Contrast volume, mL	105.8±40.8	101.6±43.1	0.66
Procedure time, min	48.8±16.6	47.6±18.1	0.76

*Significantly shorter balloon length at predilatation in the scoring balloon group (*P*=0.004).

between Δlumen area and percentage of embedded remnants (r=−0.59, *P*<0.001; Figure S2).

At baseline, half of the scaffolds in both groups had minor malapposition. There were no major malappositions in any of the groups. The percentage of malapposed struts was small in both groups and significantly lower in the scoring balloon group with 1.5% compared with 4.6% in the standard noncompliant balloon group (*P*=0.02). At baseline, malapposition volume tended to be smaller in the scoring balloon group (0.38 [0.15; 0.95] mm^2) compared with the standard noncompliant balloon group (1.07 mm^2 [0.48; 2.27] mm^2), but there was no significant difference (*P*=0.09).

At 6-month follow-up, 15.4% of the lesions treated with the scoring balloon had minor malappositions, whereas 42.9% in the standard balloon group had minor malappositions (*P*=0.009). There was significantly smaller total malapposition volume (0.0 [0.0; 0.0] versus 0.21 [0.0; 0.59]; *P*=0.009) and percentage of malapposed struts (0.0 [0.0; 0.0] versus 1.62 [0.0; 3.49]; *P*=0.004) in the scoring group compared with the standard noncompliant balloon group at 6-month follow-up. The type of malapposition did not differ between groups. Malappositions were resolved in 31.4% of the scaffolds in the scoring balloon group, compared with 48.6% in the standard noncompliant balloon group. In the scoring balloon group, 5% had persistent malapposition versus 20% in the standard balloon group. Late-acquired malapposition was seen in 15.4% of the scoring balloon group compared with 22.9% in the standard noncompliant balloon group and was often positioned at the scaffold edge and in relation to calcified plaque. Malapposition types are presented in Figure 3.

At 6-month follow-up, no scaffold area and volume were drawn since most of the struts were absorbed. OCT images of scaffold degradation are shown in Figure 2. The total number of struts was similar in the 2 groups, but there were significantly less struts per cross section in the scoring balloon group compared with the standard noncompliant balloon group after 6 months.

Intravascular Ultrasound Findings

Postprocedure and 6-month follow-up IVUS findings are presented in Tables 3 and 4 and Table S2.

Vessel Dimensions

There was no difference in vessel measurements between the 2 groups at baseline or at 6-month follow-up (Table 3). In the scoring balloon group, ΔEEM area was −0.4±1.7 mm from baseline to follow-up, compared with −1.2±1.8 mm in the standard noncompliant group (*P*=0.07). The paired analysis of mean area in the 10 mm lesion site and corresponding segment postprocedure and at 6-month follow-up are presented in Table 4. There was no significant difference in mean lumen area from postprocedure to 6-month follow-up in the scoring balloon group (8.5±1.4 versus 8.1±1.8 mm^2; *P*=0.08), whereas a significant decrease in lumen area was found in the standard noncompliant balloon group (8.2±1.7 versus 7.4±2.6 mm^2; *P*=0.009). Vessel area in the 10 mm segment corresponding to the lesion site did not change in the scoring balloon group from baseline to 6-month follow-up (16.8±2.9 versus 17.0±3.6 mm^2; *P*=0.62), but was significantly decreased (17.1±4.4 versus 15.7±4.9 mm^2; *P*<0.001) in the standard noncompliant balloon group, indicating negative remodeling.

Pattern of Remodeling

Figure 4 shows the relationship between relative change in lumen area and relative change in vessel area

Table 3. Postprocedure and 6-Month Follow-Up OCT Findings and Intravascular Ultrasound

	Baseline			6-mo follow-up		
OCT finding	**Scoring balloon**	**Standard balloon**	***P* value**	**Scoring balloon**	**Standard balloon**	***P* value**
No. of patients	40	38		39	35	
Time to 6-mo follow-up, d				185 [182; 234]	184 [182; 192]	0.29
Lumen measurement						
Minimal lumen area, mm^2	6.42±1.55	6.27±1.48	0.65	4.71±1.35	3.91±1.86	0.04
Difference in minimal lumen area (6 mo to baseline), mm^2				−1.70±1.49	−2.30±1.42	0.08
Relative change in minimal lumen area (6 mo to baseline), %				−24.8±20.4	−38.3±22.7	0.009
Mean lumen area, mm^2	8.01±1.62	7.66±2.12	0.41	7.21±1.41	6.79±2.21	0.35
Total lumen volume, mm^3	167.31±50.82	169.47±54.70	0.86	151.50±53.94	139.93±52.95	0.36
Difference in total lumen volume (6 mo to baseline), mm^3				−16.99±21.35	−25.35±28.45	0.16
Relative change in total lumen volume (6 mo to baseline), %				−10.5±11.7	−15.0±16.8	0.20
Scaffold measurement						
Total no. of analyzable struts	199.9±70.5	210.7±60.0	0.46	70.8±35.1	85.1±32.1	0.07
Mean no. of struts per cross section	9.11±0.71	9.11±0.82	1.00	3.1±1.3	3.9±1.7	0.03
Scaffold length, mm	20.8 [16.5; 24.1]	22.2 [19.2; 24.8]	0.51	20.4 [17.2; 24.0]	21.0 [17.2; 25.2]	0.69
Minimal scaffold area, mm^2	6.40±1.50	6.09±1.51	0.36			
Mean scaffold area, mm^2	7.77±1.49	7.45±1.69	0.37			
Total scaffold volume, mm^3	161.81±45.93	160.88±52.44	0.93			
Strut remnants, %						
Protruding strut remnants				58.3±22.0	54.1±26.6	0.47
Embedded strut remnants				40.6±21.1	44.9±26.9	0.45
Scaffold malapposition						
Scaffold malapposition, n (%)	20 (50.0)	21 (55.3)	0.64	6 (15.4)	15 (42.9)	0.009
Total malapposition volume, mm^3	0.38 [0.15; 0.95]	1.07 [0.48; 2.27]	0.09	0.0 [0.0; 0.0]	0.21 [0.0; 0.59]	0.009
Mean malapposition distance, mm	0.23 [0.21; 0.28]	0.30 [0.25; 0.34]	0.003	0.0 [0.0; 0.0]	0.18 [0.0; 0.4]	0.004
Percentage of malapposed struts, %	1.5 [0.6; 3.0]	4.57 [1.7; 5.8]	0.02	0.0 [0.0; 0.0]	1.6 [0.0; 3.5]	0.004
Types of incomplete stent apposition						
Resolved, n (%)				17 (48.6)	11 (31.4)	0.28
Persistent, n (%)				2 (5.0)	7 (20.0)	0.05
Late acquired, n (%)				4 (10.3)	8 (22.9)	0.14
Intravascular ultrasound						
No. of patients	40	38		39	34	
Time to 6-mo follow-up, d				183 [153; 290]	183.5 [134; 225]	0.66
Lumen measurements						
Minimal lumen area, mm^2	7.0±1.2	6.8±1.5	0.48	5.6±1.2	5.2±1.8	0.23
Difference in minimal lumen area (6 mo to baseline), mm^2				−1.4±1.5	−1.6±1.4	0.49
Vessel measurements						
EEM area at MLA site, mm^2	14.7±3.4	16.2±4.9	0.13	13.5±3.5	13.7±4.7	0.86
Mean EEM area, mm^2	16.7±2.9	17.0±4.2	0.75	16.2±3.2	15.6±4.7	0.50
Difference in mean EEM area (6 mo to baseline), mm^2				−0.4±1.7	−1.2±1.8	0.07
Total EEM volume, mm^3	361.6±97.5	383.9±130.2	0.40	353.9±120.7	336.8±110.9	0.53

EEM indicates external elastic membrane; MLA, minimal lumen area; and OCT, optical coherence tomography.

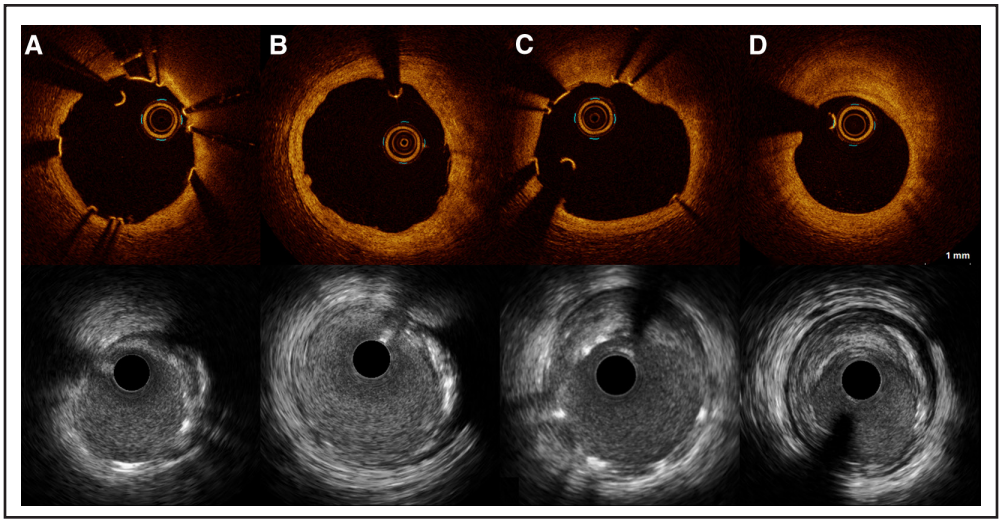

Figure 2. Intravascular images of lumen reduction after implantation of Magmaris bioresorbable scaffold.
The upper panel shows optical coherence tomography (OCT) images of minimal lumen area from baseline and the corresponding site at follow-up. The lower panel shows the matching site acquired with intravascular ultrasound (IVUS). Images (**A**) and (**B**) represent the vascular healing after lesion preparation with a scoring balloon before Magmaris bioresorbable scaffold (MgBRS) implantation. Lumen area at baseline was 7.3 mm^2 measured with OCT and 7.5 mm^2 with IVUS. Vessel area was 12.7 mm^2 at baseline (**A**). At 6-month follow-up, lumen area was 8.8 mm^2 with OCT and 8.8 mm^2 with IVUS. Vessel area was 16.0 mm^2 (**B**). Images (**C**) and (**D**) represent the vascular healing after implantation of a MgBRS in a lesion predilated with a standard noncompliant balloon. Lumen area at baseline was 8.8 mm^2 with OCT and 8.8 mm^2 with IVUS. Vessel area was 16.0 mm^2 (**C**). After 6 months, the matching site was reduced to 5.1 mm^2 measured with OCT and 5.6 mm^2 with IVUS. Vessel area was 13.8 mm^2 (**D**).

(Figure 4A), and relative change in lumen area and relative change in plaque area (Figure 4B). There was a significant positive correlation between relative change in lumen area and relative change in vessel area at the 10 mm lesion site (r, 0.72 [95% CI, 0.58–0.81]; $P<0.001$), but there was no correlation between relative change in lumen area and relative change in plaque area (r, −0.02 [95% CI, −0.25 to 0.21]; $P=0.88$).

Clinical 6-Month Follow-Up

In patients allocated to predilatation with a scoring balloon before implantation of the MgBRS, 1 patient had a target vessel revascularization not related to the scaffold-treated segment. There were no events observed corresponding to the scaffold-treated segment in the scoring balloon group. In patients treated with the standard balloon before implantation of the MgBRS, the following events were observed: 1 patient admitted with ST-segment–elevation myocardial infarction and subacute scaffold thrombosis 5 days after index procedure. This patient was only treated with aspirin for 4 days, followed by monotherapy with clopidogrel as the patient also received a novel oral anticoagulant; 1 patient died due to an intracranial hemorrhage 92 days after the index procedure.

DISCUSSION

In summary, we found that MLA assessed with OCT was significantly larger in the scoring balloon group compared with the standard noncompliant balloon group 6 months after implantation of the MgBRS. In both groups, MLA decreased from baseline to 6-month follow-up, but less MLA reduction was seen in the scoring balloon group compared with the standard noncompliant balloon group. At the lesion site, there was no change in remodeling from baseline to follow-up in the scoring balloon group, whereas negative remodeling was observed in lesions prepared with the standard noncompliant balloon. In the lesions predilated with a scoring balloon, there was significantly less malapposition at follow-up compared with the standard noncompliant balloon group.

The magnesium-based BRS was first evaluated in the DREAM 1G study (The First Generation Drug-Eluting Absorbable Metal Scafffold),[20] where a significant decrease in MLA was observed within the first 6 months (7.9±1.2 versus 5.7±1.0 mm^2) after implantation assessed with OCT. The second-generation magnesium-based BRS, MgBRS, had higher flexibility and higher radial force than the first-generation magnesium-based BRS.[21] Previous studies have investigated the vascular healing after 6 months of the magnesium-based BRS with both IVUS and OCT, but significant lumen decrease continued to occur.[6,19,22,23] Assessed with OCT, malapposition, neointimal hyperplasia, and strut coverage were near impossible to detect at follow-up because the strut remnants had lost their metallic stent-like appearance during the absorption process. Interestingly, the BIOSOLVE-II study (Biotroniks – Safety and Performance in de Novo Lesion of Native Coronary Arteries With Magmaris) reported measurable scaffold observation, such

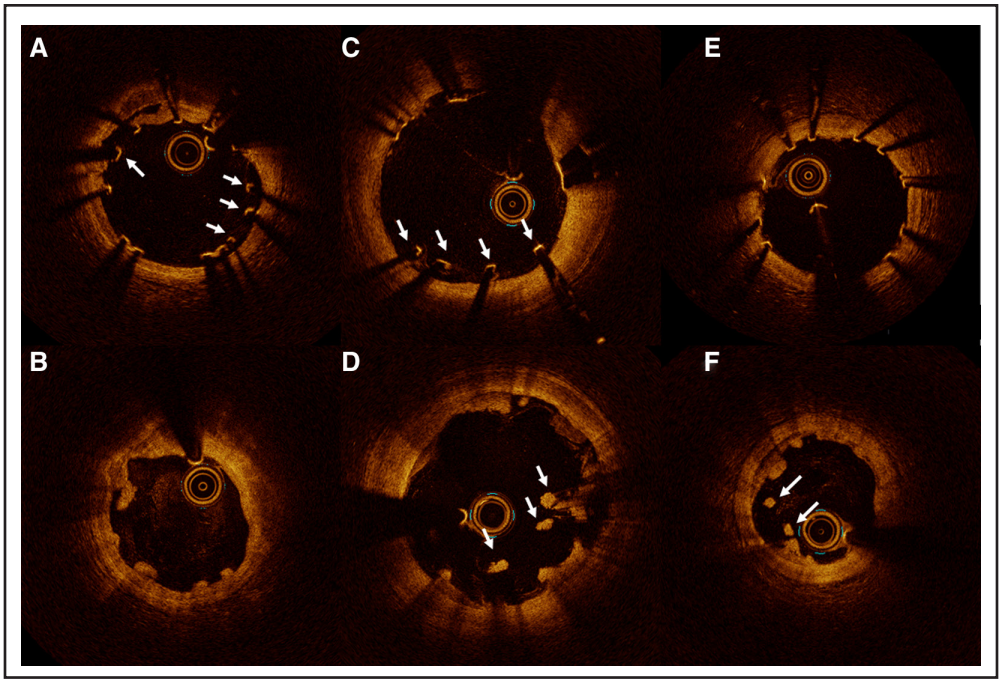

Figure 3. Optical coherence tomography images of strut remnant and malapposition types.
Upper panel represents baseline optical coherence tomography images, and lower panel represents 6-month follow-up. **A**, There are 3 malapposed struts from 3 to 5 o'clock and 1 malapposed strut at 10 o'clock (arrows). **B**, The corresponding site after 6 months revealed resolved malapposition from 3 to 5 o'clock but persistent malapposition at 10 o'clock. From 5 to 8 o'clock, protruding struts remnants are visible. **C**, Four malapposed struts are visible at baseline from 5 to 7 o'clock (arrows). **D**, At 6-month follow-up, persistent malapposition is seen in the corresponding cross section. **E**, All struts are well-apposed, but (**F**) after 6 months, acquired malapposition appears at 7 to 8 o'clock (arrows). From 1 to 3 o'clock, embedded strut remnants are visible.

as mean and minimum scaffold area and incomplete strut apposition, as visible with IVUS but not with OCT at 6-month follow-up.[22] The same pattern applied to our findings, where scaffold area detection was not possible with OCT but analyzable with IVUS at 6-month follow-up. The BIOSOLVE-II trial[22] measured smaller lumen and scaffold areas assessed with IVUS compared with OCT, which was unlike our findings with smaller lumen and scaffold measurements evaluated with OCT compared with IVUS. IVUS is often reported to overestimate lumen area compared with OCT,[17] which may explain why no difference was found between the 2 groups when using IVUS in lumen or scaffold measurements.

A third-generation magnesium-based BRS (DREAMS-3G) has been developed with a larger size range, thinner struts (99/117/147 versus 150 µm), and increased radial strength[24] compared with the MgBRS used in our study. An absolute reduction in MLA was −2.4 mm^2 (from 7.2 to 4.8 mm^2 at 6-month follow-up) for the DREAMS-3G, which was comparable to our results in the standard noncompliant balloon group with an absolute reduction of −2.3 mm^2. The scoring balloon group in our study had less absolute reduction of −1.7 mm^2. Although, we found a significant difference in MLA between the 2 groups, we still revealed lumen reduction in both groups from baseline to 6-month follow-up. Lumen reduction of 25% was considerably larger than the expected 11% lumen reduction anticipated in our power calculation.

The HONEST trial[25] comparing OCT- and angio-guided implantation with the MgBRS in a population with acute coronary syndrome found a significant reduction in MLA observed after 6 months in both groups with a relative difference of 33.2% and 22.8% in MLA, respectively. The mechanism behind lumen reduction may be due to additional postdilatation in an attempt to optimize the apposition, resulting in fracture or dismantling of the scaffold, hence reducing the radial strength.[26] In the current study, we aimed to avoid repeated postdilatations and over-dilatations to reduce the risk of scaffold fracture, which may explain the relatively low maximal pressure of 12 atm in both groups at postdilatation. Other mechanisms contributing to premature lumen loss after implantation of the MgBRS could be scaffold recoil, neointimal hyperplasia, and the impact of underlying plaque morphology and vessel remodeling.[5] The negative correlation between Δlumen area and percentage of embedded remnants may be due to the amount of neointimal hyperplasia seen in relation to embedded struts. The pattern of remodeling, with a significant correlation between change in lumen area and change in vessel area but not between change in lumen area and plaque area, indicated vessel reduction and not plaque increase as the overall reason for lumen reduction. The pattern of remodeling

Table 4. Remodeling of Lesion Segment Preprocedure and Corresponding Segment Postprocedure and at 6-Month Follow-Up Assessed With IVUS

	Scoring, n=39	Standard, n=34	*P* value
Mean lumen, mm²			
Preprocedure	5.3±1.4	4.8±1.5	0.13
Postprocedure	8.5±1.4	8.2±1.7	0.31
6-mo follow-up	8.1±1.8	7.4±2.6	0.19
Change (6 mo to baseline)	−0.4±1.5	−0.8±1.6	0.41
P value (baseline vs 6 mo)*	0.08	0.009	
Mean EEM area, mm²			
Preprocedure	13.3±3.1	13.4±4.8	0.88
Postprocedure	16.8±2.9	17.1±4.4	0.74
6-mo follow-up	17.0±3.6	15.7±4.9	0.20
Change (6 mo to baseline)	0.2±2.0	−1.4±2.0	0.001
P value (baseline vs 6 mo)*	0.62	<0.001	
Mean plaque area, mm²			
Preprocedure	7.9±2.5	8.6±3.9	0.39
Postprocedure	8.3±2.0	8.9±3.5	0.31
6-mo follow-up	8.9±2.4	8.3±3.0	0.36
Change (6 mo to baseline)	0.6±1.3	−0.7±1.9	0.002
P value (baseline vs 6 mo)*	0.007	0.06	
Mean scaffold area, mm²			
Postprocedure	9.5±1.7	9.1±1.9	0.26
6-mo follow-up	10.1±2.1	8.9±2.8	0.04
Change (6 mo to baseline)	0.6±1.9	−0.2±1.8	0.10
P value (baseline vs 6 mo)*	0.07	0.58	

EEM indicates external elastic membrane; and IVUS, intravascular ultrasound.
*Paired analysis.

was similar in the 2 groups, but the overall magnitude of vessel reduction causing lumen reduction was larger in the standard noncompliant balloon group compared with the scoring balloon group. Our results reported significantly more decrease in vessel area in lesions prepared with a standard noncompliant balloon, which was not seen in the lesions predilated with the scoring balloon. This indicates that negative remodeling and vessel shrinkage may be contributing factors for lumen loss in our study in the standard noncompliant balloon group. In the ABSORB cohort B trial (Everolimus-Eluting Bioresorbable Vascular Scaffold), dynamics of the vessel wall were investigated with IVUS after implantation of the everolimus-eluting bioresorbable ABSORB scaffold. They reported no evidence of late recoil but enlargement of the vessel, lumen, and scaffold area up to 3 years after implantation.[27] The early resorption of the MgBRS with fast loss of radial force has been suggested as a limiting factor to the device and must be investigated further.[5] The extent of scaffold recoil is a balance between elastic recoil and radial strength and can be affected by the fibrotic plaque in the coronary artery in the treated segment.[5] Optimal predilatation with a more aggressive lesion preparation could result in better vascular healing and less lumen reduction.[11] More lipid-rich plaques have been associated with less lumen loss after implantation of the MgBRS, whereas the constrictive vascular forces and rigidity of fibrotic plaque may facilitate lumen reduction.[5] Patients with acute coronary syndrome tend to have lesions with more lipid-rich plaque and positive remodeling compared with our population of patients with stable coronary syndrome, which could explain more lumen reduction than expected in the current study.

The percentage of postprocedure malapposed struts was small in our study in both groups (1.46% for the scoring balloon group and 4.57% for the standard noncompliant balloon group). As shown in previous trials,[5,19,20,22] most struts will not be visible after 6 months due to the fast scaffold absorption. Although we found up to 43% of the scaffolds with malapposition had follow-up, the percentage of malapposed struts and malapposition volume was low. Significantly less malapposition was present in the scoring balloon group compared with the standard noncompliant balloon group, which contributes to the assumption of better vascular healing after lesion preparation with a scoring balloon. To determine if these findings are a part of the natural healing process needs longer follow-up time.

Despite reported lumen loss after implantation of the MgBRS in various intravascular imaging studies,[19,22] the clinical performance is still deemed safe and efficient in several studies. Registries have reported safety and efficacy with low 1-year TLF rates of 3.3% to 5.4% and stent thrombosis rates of 0.5%, and TLF of 7.8% and scaffold thrombosis of 0.5% up to 24 months after implantation.[9,28,29] A registry study found no difference in 24-month clinical outcomes between patients with acute versus stable coronary syndromes who were treated with MgBRS.[30] Only few studies have compared the MgBRS to DES; for example, the MAGSTEMI trial (Magnesium-Based Bioresorbable Scaffold in ST-Segment–Elevation Myocardial Infarction) showed a significantly higher TLF rate in the MgBRS group after 1 year in a ST-segment–elevation myocardial infarction population.[10] However, a retrospective cohort reported similar 1-year clinical outcomes comparing the MgBRS to a biodegradable polymer DES in a non–ST-segment–elevation myocardial infarction cohort.[31] More randomized-controlled trials with long-term follow-up are needed to fully illuminate the clinical benefits or disadvantages between the new generation BRS and traditional DES.

Clinical Relevance

Besides promising clinical results from the BIOSOLVE trials supporting low scaffold thrombosis rates, the clinical use of MgBRS is still limited. The main issue has been the risk of scaffold recoil and lumen decrease. This study supports the use of intravascular imaging and the 4P implantation strategy (patient selection, pre-dilatation,

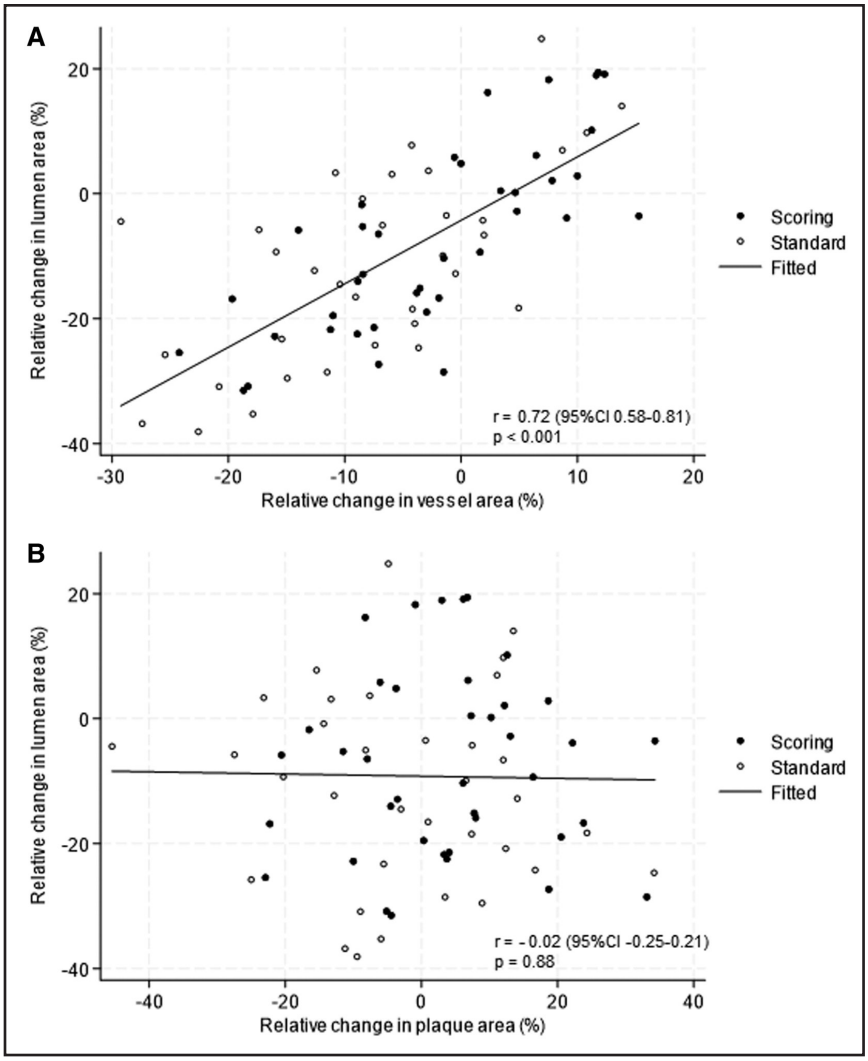

Figure 4. Pattern of remodeling at the lesion site.
A, Correlation between relative change in lumen area (%) and relative change in vessel area (%) at the lesion site. **B**, Correlation between relative change in lumen area (%) and relative change in plaque area at the lesion site.

proper sizing, and post-dilatation), focusing specifically on optimal lesion preparation to avoid recoil and scaffold restenosis. There are several potential hypotheses behind better late findings after the scoring balloon: the scoring balloon provides more controlled plaque modification compared with the standard noncompliant balloon, resulting in (1) less scarring, and thereby, less contraction of the tissue; (2) less inflammation, leading to less neointimal hyperplasia; and (3) less malapposition at both baseline and follow-up. Repeated postdilatation may result in scaffold fracture or collapse/recoil, whereas more intensive predilatation may reduce the need for overdilatation. The current study, combined with previous data on BRSs, provides a better understanding of how to optimize the implantation process of the MgBRS.

Limitations

There are some potential limitations to this study. The study was not powered to correlate clinical end points with OCT and IVUS findings. The study was conducted during the COVID-19 pandemic and was furthermore challenged by nurse strike and delivery problems of OCT catheters, which explains why the inclusion period was unexpectedly prolonged. Also, the patient and lesion selections were influenced by the limited available scaffold sizes. Finally, as blinding of the PCI operators was not possible during the procedure due to visible differences between balloons, it should be noted that more intensive optimization in the scoring balloon arm could have occurred.

Conclusions

In a selected population of patients with stable angina, lesion preparation with a scoring balloon, compared with a standard noncompliant balloon before implantation of a MgBRS, resulted in larger MLA, overall no significant remodeling, and less malapposition, whereas negative remodeling was seen in the standard noncompliant balloon group after 6 months.

ARTICLE INFORMATION

Received August 13, 2024; accepted October 7, 2024.

Affiliations

Department of Cardiology, Odense University Hospital, Denmark (K.N.H., J.T., M.N., M.H., J.E.-G., K.T.V., A.J., H.S.H., J.F.L., L.O.J.). University of Southern Denmark, Odense (K.N.H., M.N., H.S.H., J.F.L., L.O.J.). Columbia University Medical Center/New York–Presbyterian Hospital and the Cardiovascular Research Foundation, NY (A.M.).

Sources of Funding

The study is an investigator-initiated trial, and did not receive any financial support.

Disclosures

Dr Jensen has received research grants from Biotronik, OrbusNeich, Biosensors, and Terumo to her institution. The other authors report no conflicts.

Supplemental Material

Tables S1–S2
Figures S1–S2

REFERENCES

1. Azzi N, Shatila W. Update on coronary artery bioresorbable vascular scaffolds in percutaneous coronary revascularization. *Rev Cardiovasc Med*. 2021;22:137–145. doi: 10.31083/j.rcm.2021.01.225
2. Serruys PW, Katagiri Y, Sotomi Y, Zeng Y, Chevalier B, van der Schaaf RJ, Baumbach A, Smits P, van Mieghem NM, Bartorelli A, et al. Arterial remodeling after bioresorbable scaffolds and metallic stents. *J Am Coll Cardiol*. 2017;70:60–74. doi: 10.1016/j.jacc.2017.05.028
3. Ali ZA, Serruys PW, Kimura T, Gao R, Ellis SG, Kereiakes DJ, Onuma Y, Simonton C, Zhang Z, Stone GW. 2-year outcomes with the Absorb bioresorbable scaffold for treatment of coronary artery disease: a systematic review and meta-analysis of seven randomised trials with an individual patient data substudy. *Lancet*. 2017;390:760–772. doi: 10.1016/S0140-6736(17)31470-8
4. Serruys PW, Onuma Y, Ormiston JA, de Bruyne B, Regar E, Dudek D, Thuesen L, Smits PC, Chevalier B, McClean D, et al. Evaluation of the second generation of a bioresorbable everolimus drug-eluting vascular scaffold for treatment of de novo coronary artery stenosis: six-month clinical and imaging outcomes. *Circulation*. 2010;122:2301–2312. doi: 10.1161/CIRCULATIONAHA.110.970772
5. Ueki Y, Räber L, Otsuka T, Rai H, Losdat S, Windecker S, Garcia-Garcia HM, Landmesser U, Koolen J, Byrne R, et al. Mechanism of drug-eluting absorbable metal scaffold restenosis: a serial optical coherence tomography study. *Circ Cardiovasc Interv*. 2020;13:e008657. doi: 10.1161/CIRCINTERVENTIONS.119.008657
6. Haude M, Erbel R, Erne P, Verheye S, Degen H, Böse D, Vermeersch P, Wijnbergen I, Weissman N, Prati F, et al. Safety and performance of the drug-eluting absorbable metal scaffold (DREAMS) in patients with de-novo coronary lesions: 12 month results of the prospective, multicentre, first-in-man BIOSOLVE-I trial. *Lancet*. 2013;381:836–844. doi: 10.1016/S0140-6736(12)61765-6
7. Haude M, Ince H, Toelg R, Lemos PA, von Birgelen C, Christiansen EH, Wijns W, Neumann FJ, Eeckhout E, Garcia-Garcia HM, et al. Safety and performance of the second-generation drug-eluting absorbable metal scaffold (DREAMS 2G) in patients with de novo coronary lesions: three-year clinical results and angiographic findings of the BIOSOLVE-II first-in-man trial. *EuroIntervention*. 2020;15:e1375–e1382. doi: 10.4244/EIJ-D-18-01000
8. Haude M, Toelg R, Lemos PA, Christiansen EH, Abizaid A, von Birgelen C, Neumann FJ, Wijns W, Ince H, Kaiser C, et al. Sustained safety and performance of a second-generation sirolimus-eluting absorbable metal scaffold: long-term data of the BIOSOLVE-II first-in-man trial at 5 years. *Cardiovasc Revasc Med*. 2022;38:106–110. doi: 10.1016/j.carrev.2021.07.017
9. Verheye S, Wlodarczak A, Montorsi P, Torzewski J, Bennett J, Haude M, Starmer G, Buck T, Wiemer M, Nuruddin AAB, et al. BIOSOLVE-IV-registry: safety and performance of the Magmaris scaffold: 12-month outcomes of the first cohort of 1,075 patients. *Catheter Cardiovasc Interv*. 2021;98:E1–E8. doi: 10.1002/ccd.29260
10. Sabaté M, Alfonso F, Cequier A, Romaní S, Bordes P, Serra A, Iñiguez A, Salinas P, García Del Blanco B, Goicolea J, et al. Magnesium-based resorbable scaffold versus permanent metallic sirolimus-eluting stent in patients with ST-segment elevation myocardial infarction: the MAGSTEMI randomized clinical trial. *Circulation*. 2019;140:1904–1916. doi: 10.1161/CIRCULATIONAHA.119.043467
11. Miyazaki T, Latib A, Ruparelia N, Kawamoto H, Sato K, Figini F, Colombo A. The use of a scoring balloon for optimal lesion preparation prior to bioresorbable scaffold implantation: a comparison with conventional balloon predilatation. *EuroIntervention*. 2016;11:e1580–e1588. doi: 10.4244/EIJV11I14A308
12. Tearney GJ, Regar E, Akasaka T, Adriaenssens T, Barlis P, Bezerra HG, Bouma B, Bruining N, Cho JM, Chowdhary S, et al; International Working Group for Intravascular Optical Coherence Tomography (IWG-IVOCT). Consensus standards for acquisition, measurement, and reporting of intravascular optical coherence tomography studies: a report from the International Working Group for Intravascular Optical Coherence Tomography Standardization and Validation. *J Am Coll Cardiol*. 2012;59:1058–1072. doi: 10.1016/j.jacc.2011.09.079
13. Mintz GS, Guagliumi G. Intravascular imaging in coronary artery disease. *Lancet*. 2017;390:793–809. doi: 10.1016/S0140-6736(17)31957-8
14. Mintz GS, Nissen SE, Anderson WD, Bailey SR, Erbel R, Fitzgerald PJ, Pinto FJ, Rosenfield K, Siegel RJ, Tuzcu EM, et al. American College of Cardiology Clinical Expert Consensus Document on Standards for Acquisition, Measurement and Reporting of Intravascular Ultrasound Studies (IVUS). A report of the American College of Cardiology Task Force on Clinical Expert Consensus Documents. *J Am Coll Cardiol*. 2001;37:1478–1492. doi: 10.1016/s0735-1097(01)01175-5
15. Hansen KN, Maehara A, Noori M, Trøan J, Fallesen CO, Hougaard M, Ellert-Gregersen J, Veien KT, Junker A, Hansen HS, et al. Optimal lesion preparation before implantation of a Magmaris bioresorbable scaffold in patients with coronary artery stenosis: rationale, design and methodology of the OPTIMIS study. *Contemp Clin Trials Commun*. 2024;38:101260. doi: 10.1016/j.conctc.2024.101260
16. Gutiérrez-Chico JL, Cortés C, Schincariol M, Limon U, Yalcinli M, Durán-Cortés MA, Jaguszewski M. Implantation of bioresorbable scaffolds under guidance of optical coherence tomography: feasibility and pilot clinical results of a systematic protocol. *Cardiol J*. 2018;25:443–458. doi: 10.5603/CJ.a2018.0055
17. Maehara A, Matsumura M, Ali ZA, Mintz GS, Stone GW. IVUS-guided versus OCT-guided coronary stent implantation: a critical appraisal. *JACC Cardiovasc Imaging*. 2017;10:1487–1503. doi: 10.1016/j.jcmg.2017.09.008
18. Shlofmitz E, Croce K, Bezerra H, Sheth T, Chehab B, West NEJ, Shlofmitz R, Ali ZA. The MLD MAX OCT algorithm: an imaging-based workflow for percutaneous coronary intervention. *Catheter Cardiovasc Interv*. 2022;100:S7–S13. doi: 10.1002/ccd.30395
19. Fallesen CO, Antonsen L, Maehara A, Noori M, Hougaard M, Hansen KN, Ellert J, Ahlehoff O, Veien KT, Lassen JF, et al. Optical coherence tomography- versus angiography-guided magnesium bioresorbable scaffold implantation in NSTEMI patients. *Cardiovasc Revasc Med*. 2022;40:101–110. doi: 10.1016/j.carrev.2021.12.003
20. Waksman R, Prati F, Bruining N, Haude M, Böse D, Kitabata H, Erne P, Verheye S, Degen H, Vermeersch P, et al. Serial observation of drug-eluting absorbable metal scaffold: multi-imaging modality assessment. *Circ Cardiovasc Interv*. 2013;6:644–653. doi: 10.1161/CIRCINTERVENTIONS.113.000693
21. Waksman R, Zumstein P, Pritsch M, Wittchow E, Haude M, Lapointe-Corriveau C, Leclerc G, Joner M. Second-generation magnesium scaffold Magmaris: device design and preclinical evaluation in a porcine coronary artery model. *EuroIntervention*. 2017;13:440–449. doi: 10.4244/EIJ-D-16-00915
22. Haude M, Ince H, Abizaid A, Toelg R, Lemos PA, von Birgelen C, Christiansen EH, Wijns W, Neumann FJ, Kaiser C, et al. Safety and performance of the second-generation drug-eluting absorbable metal scaffold in patients with de-novo coronary artery lesions (BIOSOLVE-II): 6 month results of a prospective, multicentre, non-randomised, first-in-man trial. *Lancet*. 2016;387:31–39. doi: 10.1016/S0140-6736(15)00447-X
23. Tovar Forero MN, van Zandvoort L, Masdjedi K, Diletti R, Wilschut J, de Jaegere PP, Zijlstra F, Van Mieghem NM, Daemen J. Serial invasive imaging follow-up of the first clinical experience with the Magmaris magnesium bioresorbable scaffold. *Catheter Cardiovasc Interv*. 2020;95:226–231. doi: 10.1002/ccd.28304
24. Haude M, Wlodarczak A, van der Schaaf RJ, Torzewski J, Ferdinande B, Escaned J, Iglesias JF, Bennett J, Toth G, Joner M, et al. Safety and performance of the third-generation drug-eluting resorbable coronary magnesium scaffold system in the treatment of subjects with de novo coronary artery lesions: 6-month results of the prospective, multicenter BIOMAG-I first-in-human study. *EClinicalMedicine*. 2023;59:101940. doi: 10.1016/j.eclinm.2023.101940
25. Fallesen CO, Maehara A, Antonsen L, Nørregaard Hansen K, Noori M, Flensted Lassen J, Junker A, Hansen HS, Okkels Jensen L. Coronary artery healing process after bioresorbable scaffold in patients with non-ST-segment

elevation myocardial infarction: rationale, design, and methodology of the HONEST study. *Cardiology*. 2021;146:161–171. doi: 10.1159/000512417
26. Barkholt T, Webber B, Holm NR, Ormiston JA. Mechanical properties of the drug-eluting bioresorbable magnesium scaffold compared with polymeric scaffolds and a permanent metallic drug-eluting stent. *Catheter Cardiovasc Interv*. 2020;96:E674–Ee82.
27. Serruys PW, Onuma Y, Garcia-Garcia HM, Muramatsu T, van Geuns RJ, de Bruyne B, Dudek D, Thuesen L, Smits PC, Chevalier B, et al. Dynamics of vessel wall changes following the implantation of the absorb everolimus-eluting bioresorbable vascular scaffold: a multi-imaging modality study at 6, 12, 24 and 36 months. *EuroIntervention*. 2014;9:1271–1284. doi: 10.4244/EIJV9I11A217
28. Galli S, Troiano S, Palloshi A, Rapetto C, Pisano F, Aprigliano G, Leoncini M, Ravagnani P, Del Maestro M, Montorsi P. Sustained safety and efficacy of magnesium reabsorbable scaffold: 2-year follow-up analysis from first magmaris multicenter Italian registry. *Cardiovasc Revasc Med*. 2022;41:69–75. doi: 10.1016/j.carrev.2022.01.020
29. Haude M, Ince H, Kische S, Abizaid A, Tölg R, Alves Lemos P, Van Mieghem NM, Verheye S, von Birgelen C, Christiansen EH, et al; BIOSOLVE-II and III investigators. Safety and clinical performance of a drug eluting absorbable metal scaffold in the treatment of subjects with de novo lesions in native coronary arteries: pooled 12-month outcomes of BIOSOLVE-II and BIOSOLVE-III. *Catheter Cardiovasc Interv*. 2018;92:E502–E511. doi: 10.1002/ccd.27680
30. Galli S, Troiano S, Palloshi A, Rapetto C, Pisano F, Aprigliano G, Leoncini M, Ravagnani P, Del Maestro M, Montorsi P. Comparison of acute versus stable coronary syndrome in patients treated with the Magmaris scaffold: two-year results from the Magmaris Multicenter Italian Registry. *Cardiovasc Revasc Med*. 2023;57:53–59. doi: 10.1016/j.carrev.2023.06.022
31. Rola P, Włodarczak A, Włodarczak S, Barycki M, Szudrowicz M, Łanocha M, Furtan L, Woźnica K, Kulczycki JJ, Jaroszewska-Pozorska J, et al. Magnesium Bioresorbable Scaffold (BRS) Magmaris vs Biodegradable Polymer DES Ultimaster in NSTE-ACS Population-12-Month Clinical Outcome. *J Interv Cardiol*. 2022;2022:5223317. doi: 10.1155/2022/5223317